Spectroscopic factors from Faddeev calculations in ^{3}He and related topics

ELVIRA MOYA DE GUERRA

CSIC
MADRID
SPAIN

R. Álvarez-Rodríguez
E. Garrido
P. Sarriguren
J. M. Udías

J. A. Caballero
T. W. Donnelly

A. Antonov
M. Gaidarov

I Spectroscopic factors from “exact” calculations.
The ^{3}He$(e, e'p)^2$H reaction.

II Spectroscopic factors from fits to mean field $(e, e'p)$ reactions in ^{40}Ca, ^{208}Pb.

III Superscaling and high momentum contributions.

Nuclear Current

$$J^\mu(\boldsymbol{q}) = \int d\boldsymbol{x} e^{i\boldsymbol{q}\cdot\boldsymbol{x}} \langle \Psi_F | \hat{J}^\mu(\boldsymbol{x}) | \Psi_I \rangle$$

$$J^\mu(\boldsymbol{q}) = \int d\boldsymbol{r}_1 d\boldsymbol{r}_2 d\boldsymbol{r}_3 e^{i\boldsymbol{q}\cdot\boldsymbol{r}_3} \Psi_d^\dagger(\boldsymbol{r}_1,\boldsymbol{r}_2)\phi_p^\dagger(\boldsymbol{r}_3)\widehat{j}_\mu(\boldsymbol{q})\Psi_I(\boldsymbol{r}_1,\boldsymbol{r}_2,\boldsymbol{r}_3),$$

With $\boldsymbol{x} = \sqrt{\frac{1}{2}}(\boldsymbol{r}_1 - \boldsymbol{r}_2)$ and $\boldsymbol{y} = \sqrt{\frac{2}{3}}\left(\boldsymbol{r}_3 - \frac{\boldsymbol{r}_1+\boldsymbol{r}_2}{2}\right) = \sqrt{\frac{2}{3}}\left(\boldsymbol{r}_3 - \boldsymbol{R}_d\right)$

$$\begin{aligned}\Psi_d(\boldsymbol{r}_1,\boldsymbol{r}_2) &= e^{i\boldsymbol{P_d}\cdot\boldsymbol{R_d}}\Psi_d(\boldsymbol{x}) \\ \Psi_I(\boldsymbol{r}_1,\boldsymbol{r}_2,\boldsymbol{r}_3) &= e^{i\boldsymbol{P}\cdot\boldsymbol{R}}\Psi_{He}(\boldsymbol{x},\boldsymbol{y})\end{aligned}$$

$$J^\mu(\boldsymbol{q}) = (2\pi)^3\delta^{(3)}(\boldsymbol{P} + \boldsymbol{q} - \boldsymbol{P}_d - \boldsymbol{p})J^\mu_{int}(\boldsymbol{q})$$

$$J^\mu_{int}(\boldsymbol{q}) = \left(\frac{3}{2}\right)^{3/2} \int d\boldsymbol{y} e^{i\sqrt{\frac{3}{2}}\boldsymbol{y}\cdot\boldsymbol{q}} \phi_p^\dagger(\boldsymbol{y})\widehat{j}^\mu(\boldsymbol{q})\tilde{\phi}(\boldsymbol{y})$$

$$\frac{d\sigma}{d\varepsilon_f d\Omega_e d\Omega_p} = \frac{\alpha^2}{q^4} \frac{1}{8(2\pi)^3 k_i \cdot P_I} \frac{|\boldsymbol{p}||\boldsymbol{k}_f|}{M_I} f_r^{-1} \eta_{\mu\nu} W^{\mu\nu}$$

$$W^{\mu\nu} = \overline{\sum_I} \sum_F J^\mu_{int} J^\nu_{int}$$

$$\rho(p_m) = \frac{d\sigma}{d\varepsilon_f d\Omega_e d\Omega_p} \frac{1}{f_r^{-1} |\boldsymbol{p}| E_p \sigma_{ep}}$$

Nuclear current, overlap function and spectroscopic factor

$$J^\mu_{int}(\boldsymbol{q}) = \left(\frac{3}{2}\right)^{3/2} \int d\boldsymbol{y} e^{i\sqrt{\frac{3}{2}}\boldsymbol{y}\cdot\boldsymbol{q}} \phi_p^\dagger(\boldsymbol{y}) \widehat{j}^\mu(\boldsymbol{q}) \tilde{\phi}(\boldsymbol{y})$$

$$\tilde{\phi}(\boldsymbol{y}) = 2^{3/2} \int d\boldsymbol{x} \Psi_d^\dagger(\boldsymbol{x}) \Psi_{He}(\boldsymbol{x}, \boldsymbol{y})$$

$$S = \left(\frac{3}{2}\right)^{3/2} \int d\boldsymbol{y} |\tilde{\phi}(\boldsymbol{y})|^2$$

Spectroscopic factors (S) .

	S
v18 fitb	0.65625
v18 no3b	0.66619
v8 exp2	0.63911
v8 fitb2	0.63695
v8 no3b2	0.64142
gaus expmy	0.65480
gaus fitmy	0.65367
gaus no3bmy	0.65635

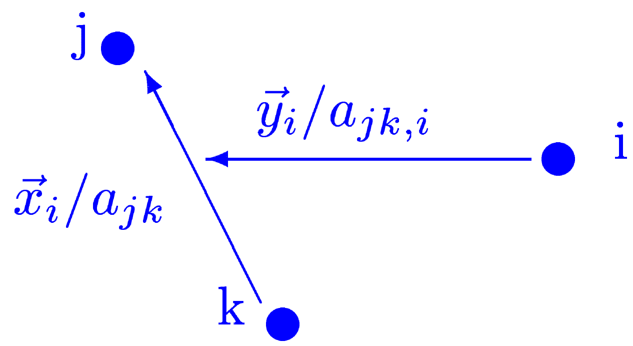

$$\Psi_{He} = \sum_{i=1}^{3} \psi^{(i)}(\boldsymbol{x}_i, \boldsymbol{y}_i)$$

Fadeev equations:

$$(T-E)\psi^{(i)}(\boldsymbol{x}_i, \boldsymbol{y}_i)+V_i(x_i)\left(\psi^{(i)}(\boldsymbol{x}_i, \boldsymbol{y}_i) + \psi^{(j)}(\boldsymbol{x}_j, \boldsymbol{y}_j) + \psi^{(k)}(\boldsymbol{x}_k, \boldsymbol{y}_k)\right) = 0$$

Hyperspherical coordinates: $\rho = \sqrt{x_i^2 + y_i^2}$ and $\alpha_i = \arctan(x_i/y_i)$.

$$\psi^{(i)}(\boldsymbol{x}_i, \boldsymbol{y}_i) = \frac{1}{\rho^{5/2}} \sum_n f_n(\rho) \phi_n^{(i)}(\rho, \Omega_i),$$

Angular part:

$$\widehat{\Lambda}^2 \phi_n^{(i)} + \frac{2m\rho^2}{\hbar^2} V_i(\phi_n^{(i)} + \phi_{nJM}^{(j)} + \phi_n^{(k)}) = \lambda_n(\rho) \phi_n^{(i)} \ ,$$

$$\phi_n^{(i)}(\rho, \Omega_i) = \sum_{K \ell_x \ell_y L s_x S} C^{(i)}_{nK\ell_x\ell_y L s_x S}(\rho) \left[Y^{KL}_{\ell_x \ell_y}(\Omega_i) \otimes \chi^{(i)}_{s_x s_y S} \right]^{JM}$$

Radial part:

$$\left(-\frac{d^2}{d\rho^2} - \frac{2mE}{\hbar^2} + \frac{1}{\rho^2} \left(\lambda_n(\rho) + \frac{15}{4} \right) \right) f_n(\rho) =$$
$$\sum_{nn'} \left(2P_{nn'}(\rho) \frac{d}{d\rho} + Q_{nn'}(\rho) \right) f_{n'}(\rho)$$

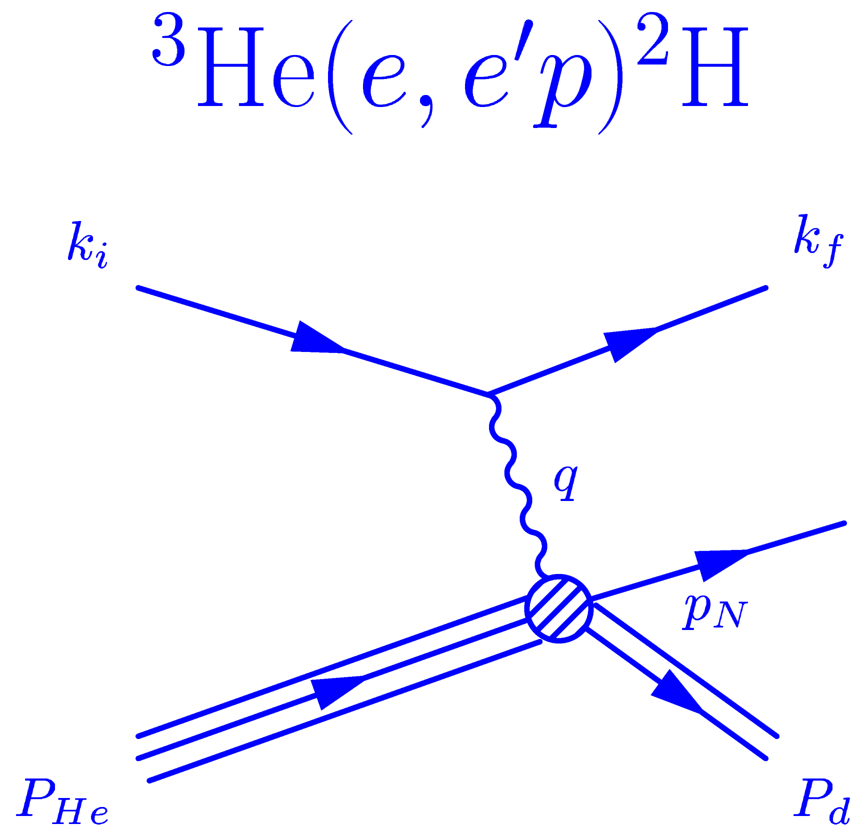

$^{3}\mathrm{He}(e,e'p)^{2}\mathrm{H}$
k_i
k_f
q
p_N
P_{He}
P_d

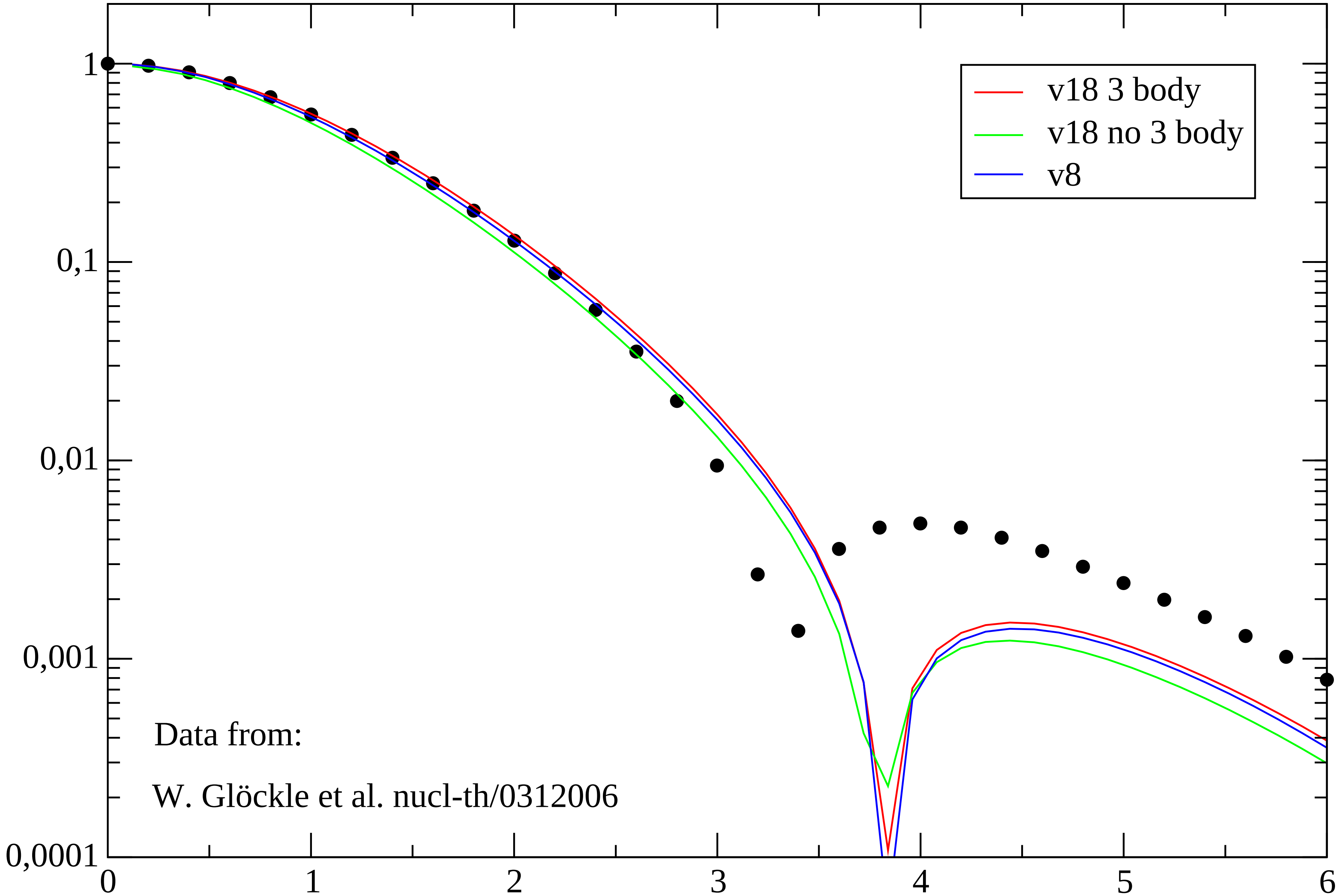

v18 3 body
v18 no 3 body
v8
Data from:
W. Glöckle et al. nucl-th/0312006
1
0,1
0,01
0,001
0,0001
0
1
2
3
4
5
6

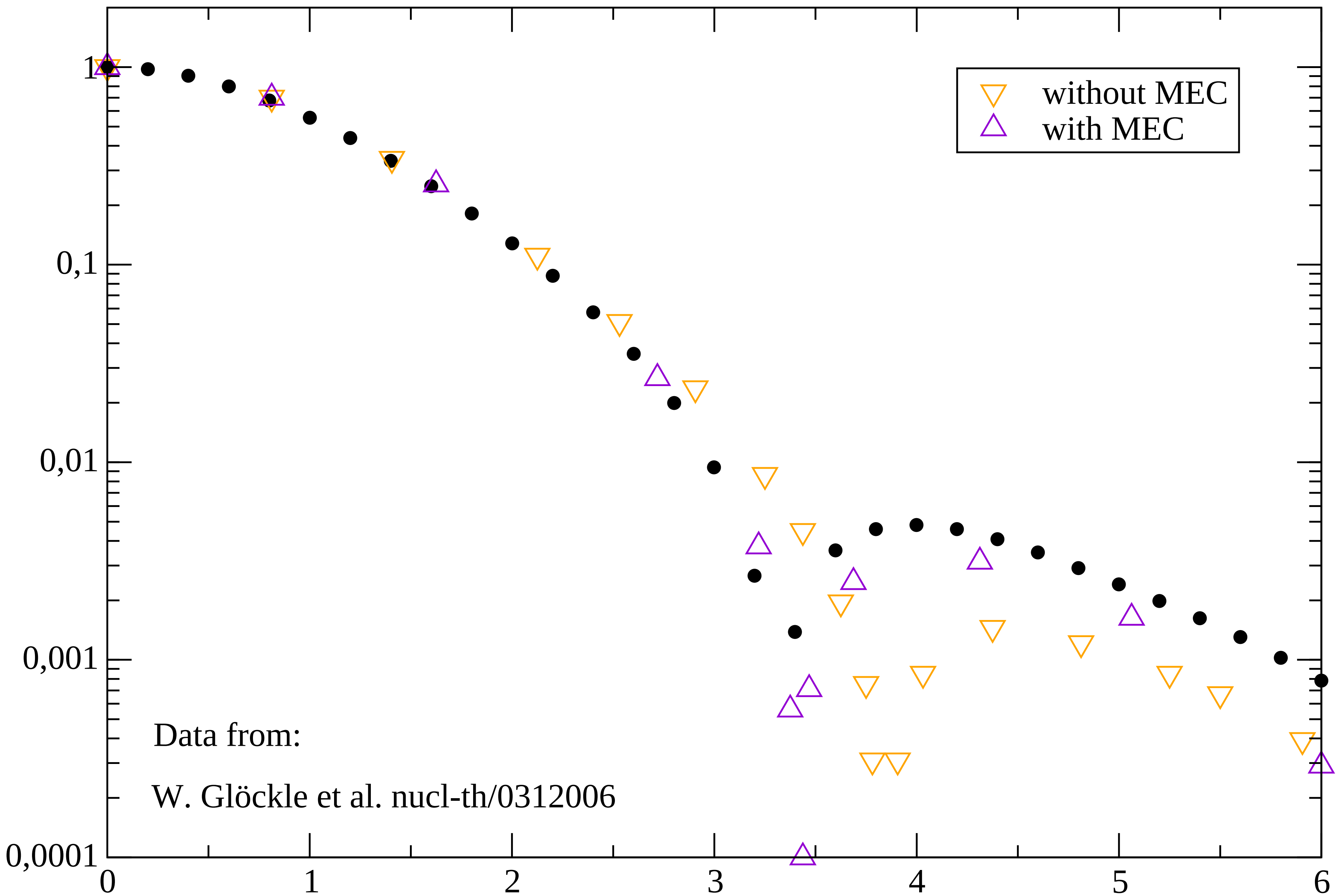

without MEC
with MEC
1
0,1
0,01
0,001
0,0001
0
1
2
3
4
5
6
Data from:
W. Glöckle et al. nucl-th/0312006

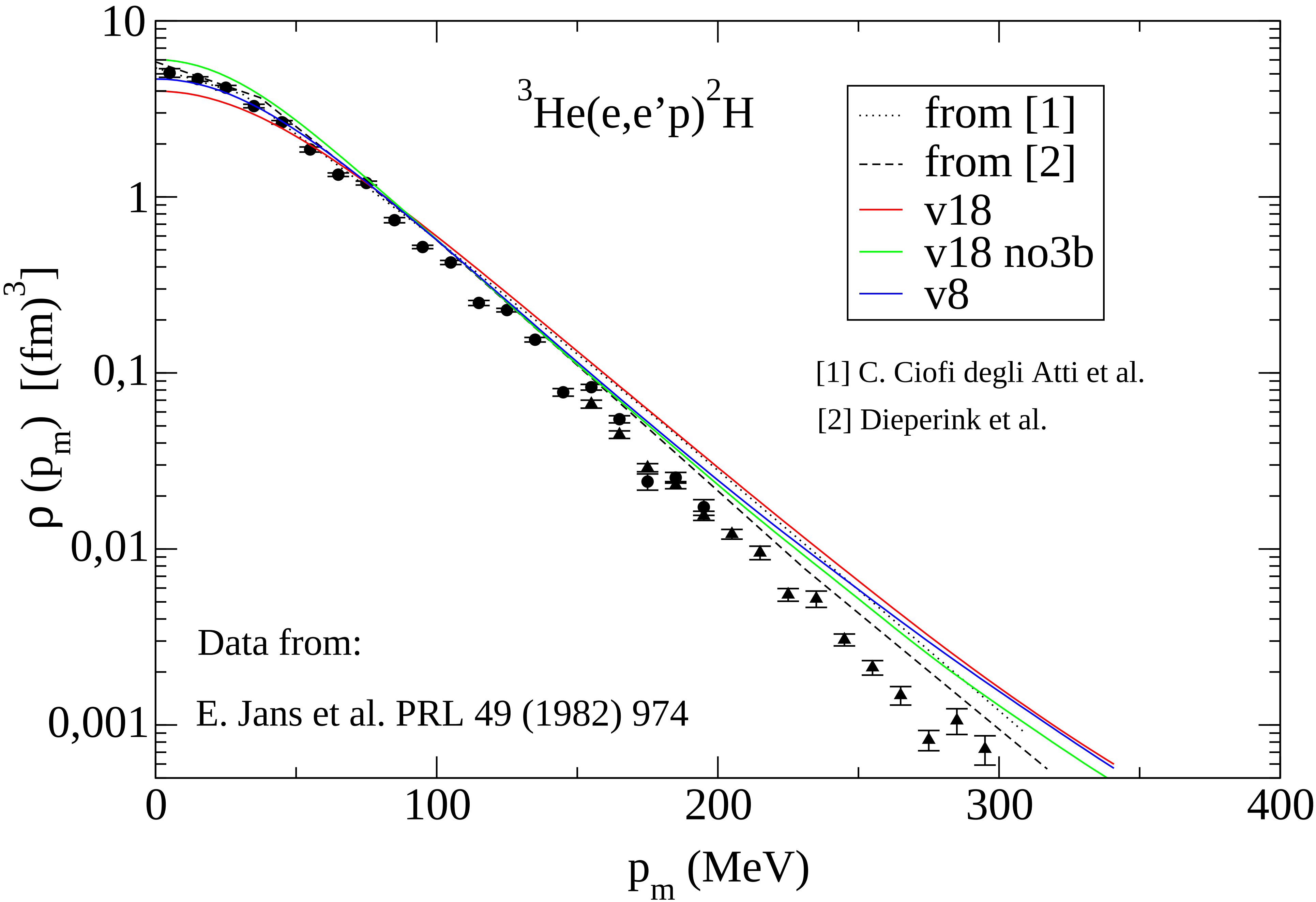

$^3He(e,e'p)^2H$
from [1]
from [2]
v18
v18 no3b
v8
[1] C. Ciofi degli Atti et al.
[2] Dieperink et al.
Data from:
E. Jans et al. PRL 49 (1982) 974
$\rho\,(p_m)$ [(fm)^3]
10
1
0,1
0,01
0,001
0
100
200
300
400
p_m (MeV)

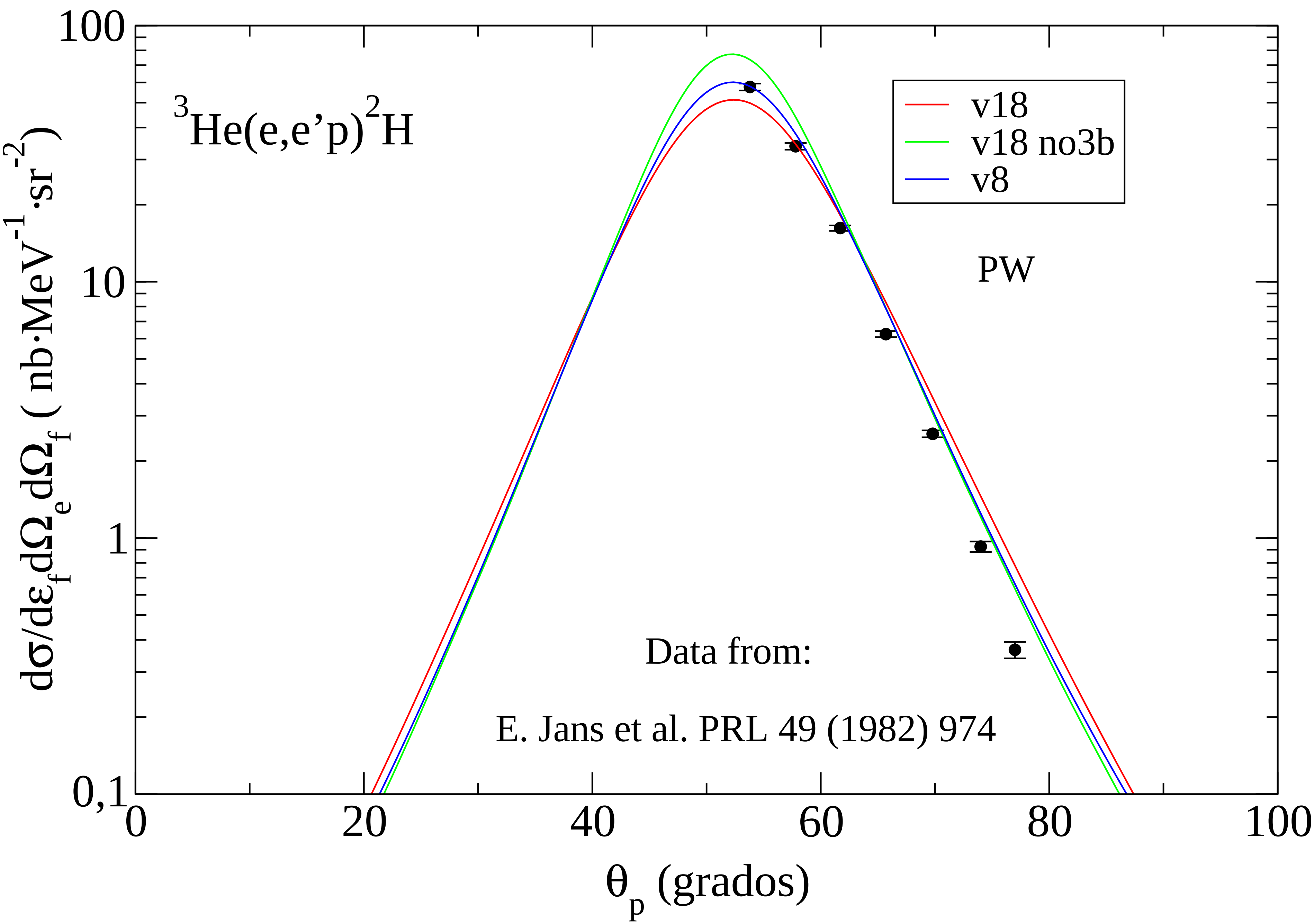

^{3}He(e,e'p)^{2}H
v18
v18 no3b
v8
PW
Data from:
E. Jans et al. PRL 49 (1982) 974
$d\sigma/d\varepsilon_f d\Omega_e d\Omega_f$ (nb·MeV^{-1}·sr^{-2})
θ_p (grados)
100
10
1
0,1
0
20
40
60
80
100

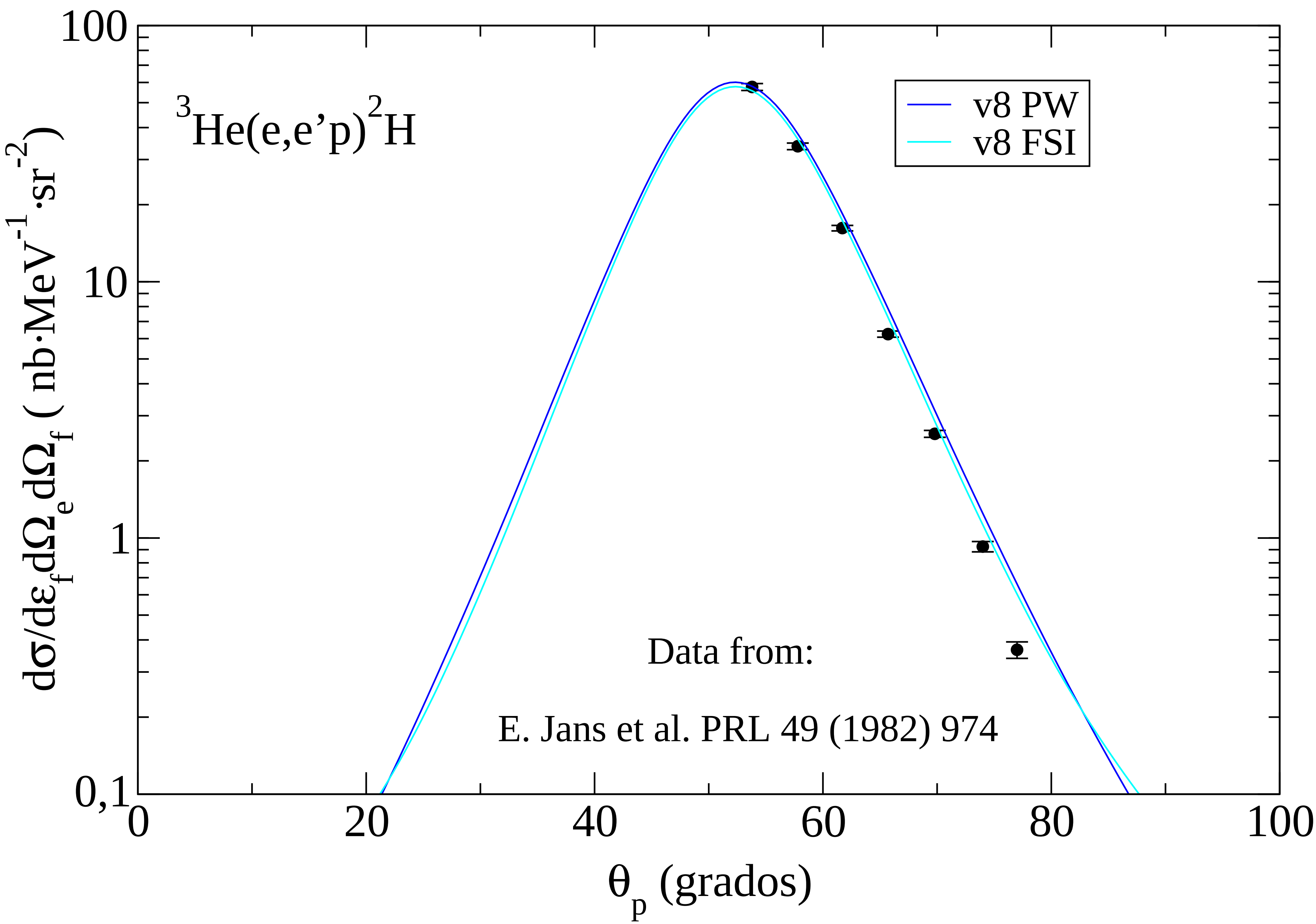

100
10
1
0,1
0
20
40
60
80
100
^{3}He(e,e'p)^{2}H
v8 PW
v8 FSI
Data from:
E. Jans et al. PRL 49 (1982) 974
$d\sigma/d\varepsilon_f d\Omega_e d\Omega_f$ (nb·MeV^{-1}·sr^{-2})
θ_p (grados)

RELATIVISTIC CALCULATION

- Nuclear Current:

$$J^{\mu}_{N}(\omega, \boldsymbol{q}) = \int d\boldsymbol{y} e^{i\boldsymbol{q}\cdot\boldsymbol{y}} \bar{\Psi}_F(\boldsymbol{y}) \hat{J}^{\mu}_{N} \Psi_B(\boldsymbol{y})$$

Free Nucleon: $\hat{J}^{\mu} = F_1(q^2)\gamma^{\mu} + i\kappa F_2(q^2)\dfrac{\sigma^{\mu\nu}q_{\nu}}{2M}$

- Wave Functions: Solutions of Dirac equation

$$\left[i\vec{\alpha}\cdot\vec{\nabla} - \beta(M-S) + E - V \right] \Psi = 0$$

- Ψ_B: Selfconsistent solution (relativistic Hartree calculation)
- Ψ_F: Continuum solution. Optical potential fitted to elastic proton scattering data (energies in the range: 15 MeV – 1 GeV)

APPLICATION TO $p < 300$ MEV (NIKHEF)

COMPARISON WITH EXPERIMENT

LOW MOMENTUM, $p \leq 300$ MeV/c

- Spectroscopic factors are larger in the relativistic analysis: ^{208}Pb: occupation numbers obtained by comparison with the $(e, e'p)$ cross section data measured at NIKHEF-K (88)

Shell	$3s_{1/2}$	$2d_{3/2}$	$1h_{11/2}$	$2d_{5/2}$	$1g_{7/2}$
Non-relativistic (NIKHEF)	0.55	0.57	0.58	0.54	0.26
Relativistic (CSIC)	0.70	0.73	0.64	0.60	0.30

- The shape of the cross section is well described in relativistic and non-relativistic analyses

Why increased absorption?

Nucleon Wave Functions

Scalar, $S = S(r)$, and vector, $V_\mu = (V(r), 0)$, potentials

Dirac equation with S-V potentials

$$\left[\gamma_0 \widetilde{E} - \boldsymbol{\gamma} \cdot \boldsymbol{p} - \widetilde{M}\right] \Psi^\kappa = 0 \quad , \quad \Psi^\kappa = \begin{pmatrix} \Psi^\kappa_{up} \\ \Psi^\kappa_{down} \end{pmatrix}$$

$$\widetilde{M} = M - S \quad , \qquad \widetilde{E} = E - V,$$

$$A_\pm = \widetilde{E} \pm \widetilde{M} \quad , \qquad A_+ A_- = \widetilde{E}^2 - \widetilde{M}^2 = K^2 + 2MU_{central}$$

$$\text{ESE} \begin{cases} \left[\nabla^2 + \dfrac{1}{A_+}\dfrac{\partial A_+}{\partial r}\left(\dfrac{\boldsymbol{\sigma} \cdot \boldsymbol{l}}{r} - \dfrac{\partial}{\partial r}\right) + A_+ A_-\right] \Psi^\kappa_{up}(r) = 0 \\ \left[\nabla^2 + \dfrac{1}{A_-}\dfrac{\partial A_-}{\partial r}\left(\dfrac{\boldsymbol{\sigma} \cdot \boldsymbol{l}}{r} - \dfrac{\partial}{\partial r}\right) + A_+ A_-\right] \Psi^\kappa_{down}(r) = 0 \end{cases}$$

$$\Psi^\kappa(r) \to \Psi^\kappa_{up}(r) \to K(r)\phi(r) \quad , \quad K^2(r) = 1 - \frac{V + S}{E + M}$$

$$\Psi^\kappa_{up} = \frac{\boldsymbol{\sigma} \cdot \boldsymbol{p}}{\widetilde{E} - \widetilde{M}} \Psi^\kappa_{down}$$

$$\Psi^\kappa_{down} = \frac{\boldsymbol{\sigma} \cdot \boldsymbol{p}}{\widetilde{E} + \widetilde{M}} \Psi^\kappa_{up}$$

$$|\kappa| = j + \frac{1}{2}$$

$$\kappa > 0, \; j = \kappa - \frac{1}{2} = l^4 - \frac{1}{2}$$

$$\kappa < 0, \; j = -\kappa - \frac{1}{2} = l^4 + \frac{1}{2}$$

$$l_d = l_u \pm 1$$

$$\Psi^\kappa_{up}(r) \sim \left[Y_{l^u} \otimes \chi_{1/2}\right]_j$$

$$\Psi^\kappa_{down}(r) \sim \left[Y_{l^d} \otimes \chi_{1/2}\right]_j$$

Why higher momentum components?

RPWIA (NO FACTORIZATION)

$$\frac{d^5\sigma}{d\Omega_e d\varepsilon' d\Omega_N} = \frac{2\alpha^2}{Q^4}\left(\frac{\varepsilon'}{\varepsilon}\right)\frac{p_N M_B}{M_A f_{rec}} 2\overline{\sum}|\mathcal{M}|^2,$$

with

$$\mathcal{M} = j^e_\mu J^\mu_N,$$

$$J^\mu_N = \bar{u}_{\sigma_N}(\mathbf{p}_N)\hat{J}^\mu_N \underbrace{\uparrow}_{\sum_s (u\bar{u} - v\bar{v}) = 1} \Psi^{m_b}_b(\mathbf{p}) \qquad = \langle J^\mu_N \rangle_u - \langle J^\mu_N \rangle_v,$$

$$\langle J^\mu_N \rangle_u \;\equiv\; \langle J^\mu \rangle_u = \sum_s \bar{u}(\mathbf{p}_N, s_N)\hat{J}^\mu u(\mathbf{p}, s)\left[\bar{u}(\mathbf{p}, s)\Psi^{m_b}_b(\mathbf{p})\right]$$

$$\langle J^\mu_N \rangle_v \;\equiv\; \langle J^\mu \rangle_v = \sum_s \bar{u}(\mathbf{p}_N, s_N)\hat{J}^\mu v(\mathbf{p}, s)\left[\bar{v}(\mathbf{p}, s)\Psi^{m_b}_b(\mathbf{p})\right]$$

Comparison of RPWIA and PWIA

$$\frac{d^5\sigma}{d\Omega_e d\varepsilon' d\Omega_N} = \frac{p_N M M_B}{M_A f_{rec}} \left[\underline{\sigma^{ep}_{uu} N_{uu}(p)} + \sigma^{ep}_{vv} N_{vv}(p) + \sigma^{ep}_{uv} N_{uv}(p) \right]$$

$$\sigma^{ep}_{uu} = \frac{2\alpha^2}{Q^4}\frac{\varepsilon'}{\varepsilon}\eta_{\mu\nu}\mathcal{W}^{\mu\nu} = \sigma^{ep} \xrightarrow{\text{PWIA}} \sigma^{ep}$$

$$\sigma^{ep}_{vv} = \frac{2\alpha^2}{Q^4}\frac{\varepsilon'}{\varepsilon}\eta_{\mu\nu}\mathcal{Z}^{\mu\nu} \longrightarrow 0$$

$$\sigma^{ep}_{uv} = \frac{2\alpha^2}{Q^4}\frac{\varepsilon'}{\varepsilon}\eta_{\mu\nu}\mathcal{N}^{\mu\nu} \longrightarrow 0$$

Can we finger out genuine relativistic effects?

$$J^\mu = (\rho_L, \boldsymbol{J}_T)$$

$$\left(\frac{d^5\sigma}{dE'_0 d\Omega_{p'_0} d\Omega_{p'}} \right)^{(e,e'p)} = (2\pi)^3 \frac{p' E' f_{rec}}{M_h}$$

$$\sigma_M \left(V_L W_L + V_T W_T + V_{LT} W_{LT} + V_{TT} W_{TT} \right)$$

$$\sim \sigma_{ep} \left(v_L R^L + v_T R^T + v_{LT} R^{LT} v_{TT} R^{TT} \right)$$

the equivalent Schrödinger equation:

$$\left[-\frac{\nabla^2}{2M} - U_{\rm DEB}\right] \phi(\mathbf{r}) = E_{\rm nr}\phi(\mathbf{r}) \, ,$$

with $E_{\rm nr} = (E^2 - M^2)/2M$ and $\phi(\mathbf{r})$ a bispinoı

V_c & V_{so} are similar

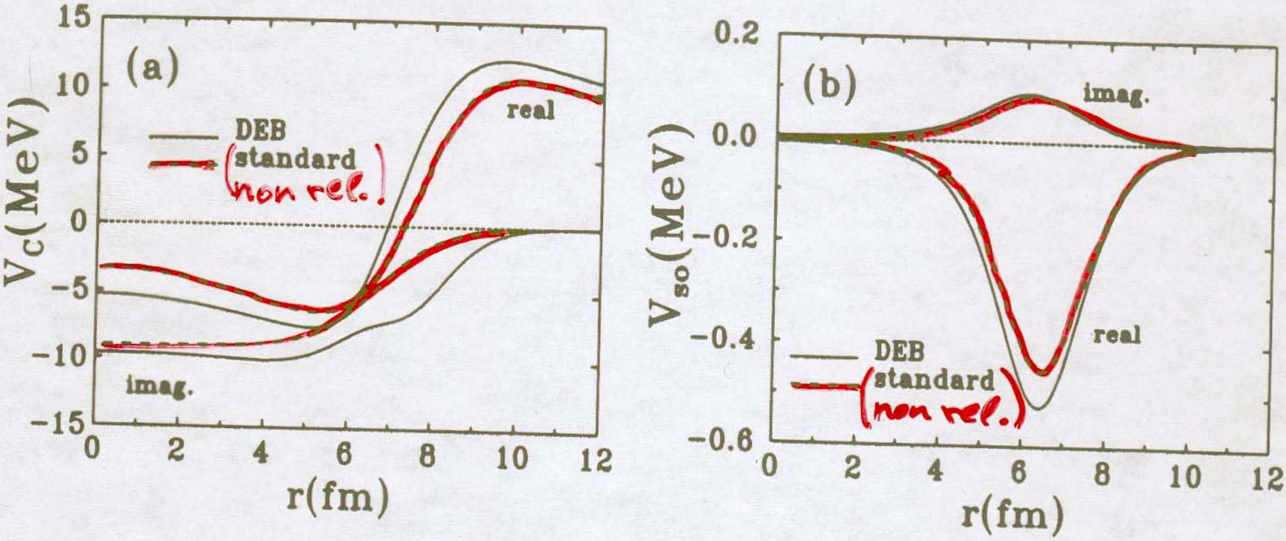

BUT !

$$\Psi_{\rm up}(\mathbf{r}) = \underline{K(r)}\phi(\mathbf{r})$$

$$K(r) = A^{1/2}(r)$$

$\Downarrow$

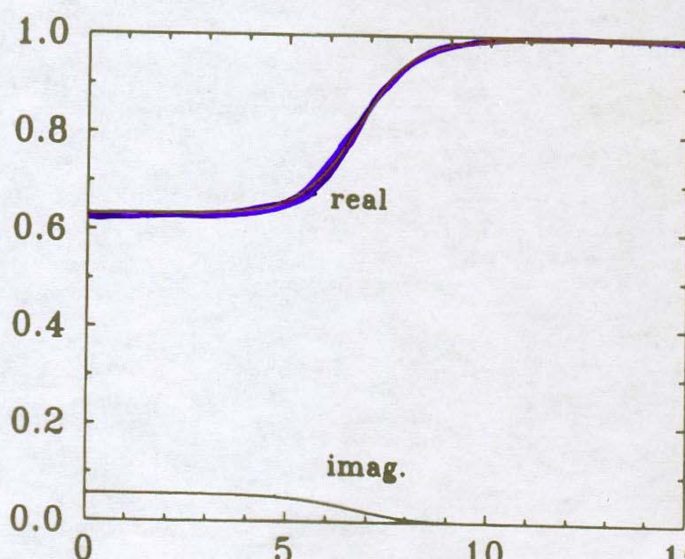

NEW DATA AT **HIGH P_m** (1995)

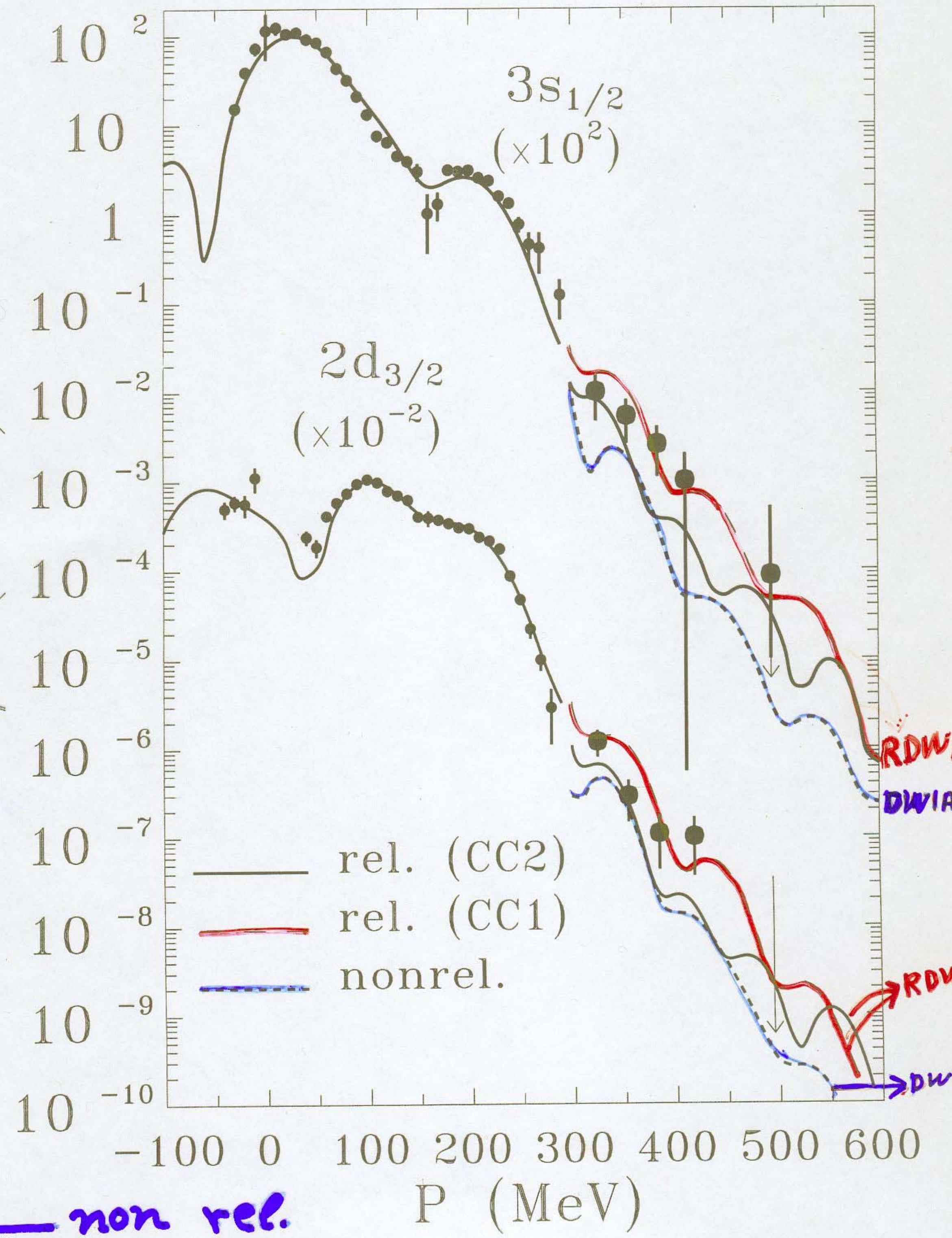

— non rel.

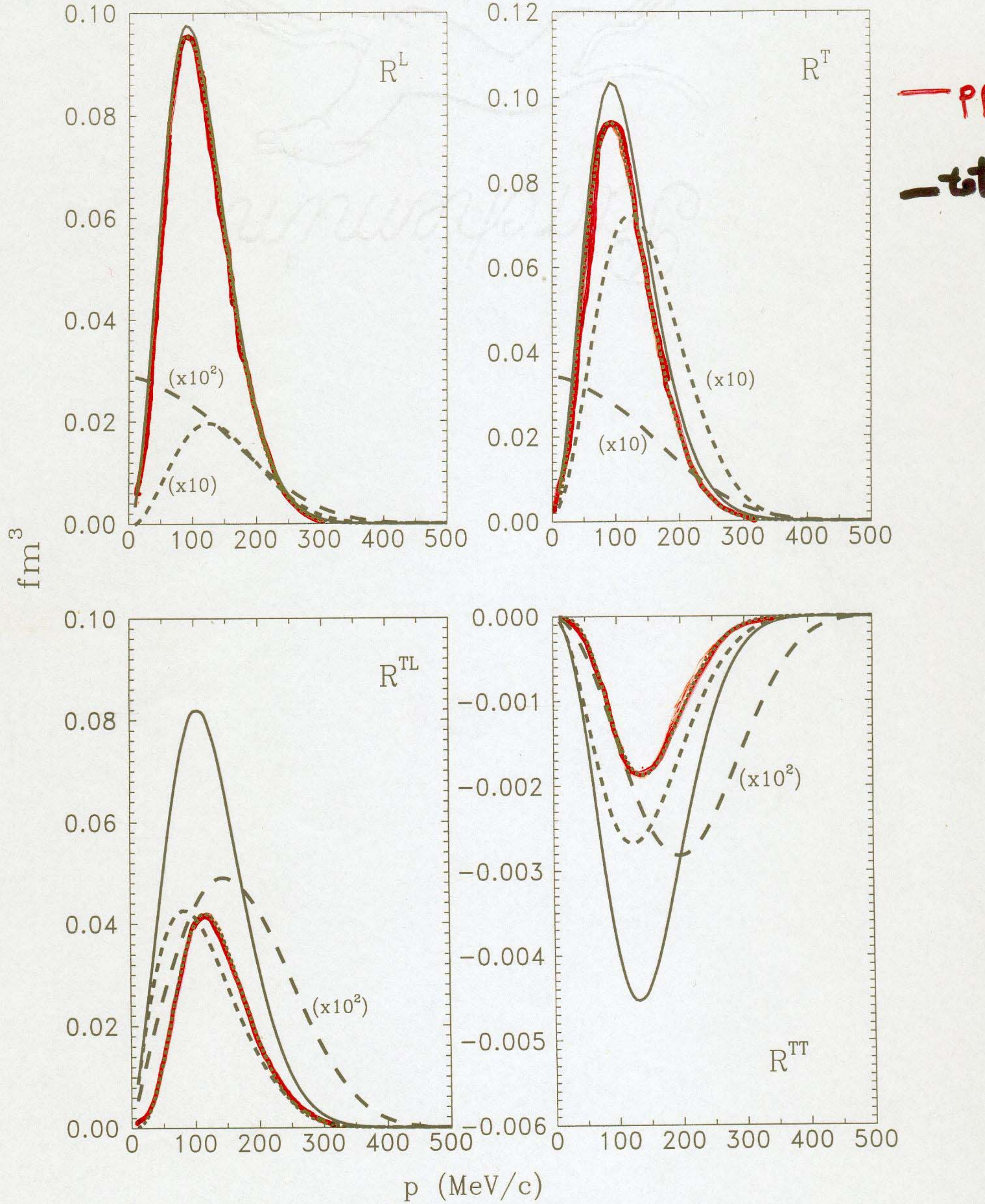

Figure 10

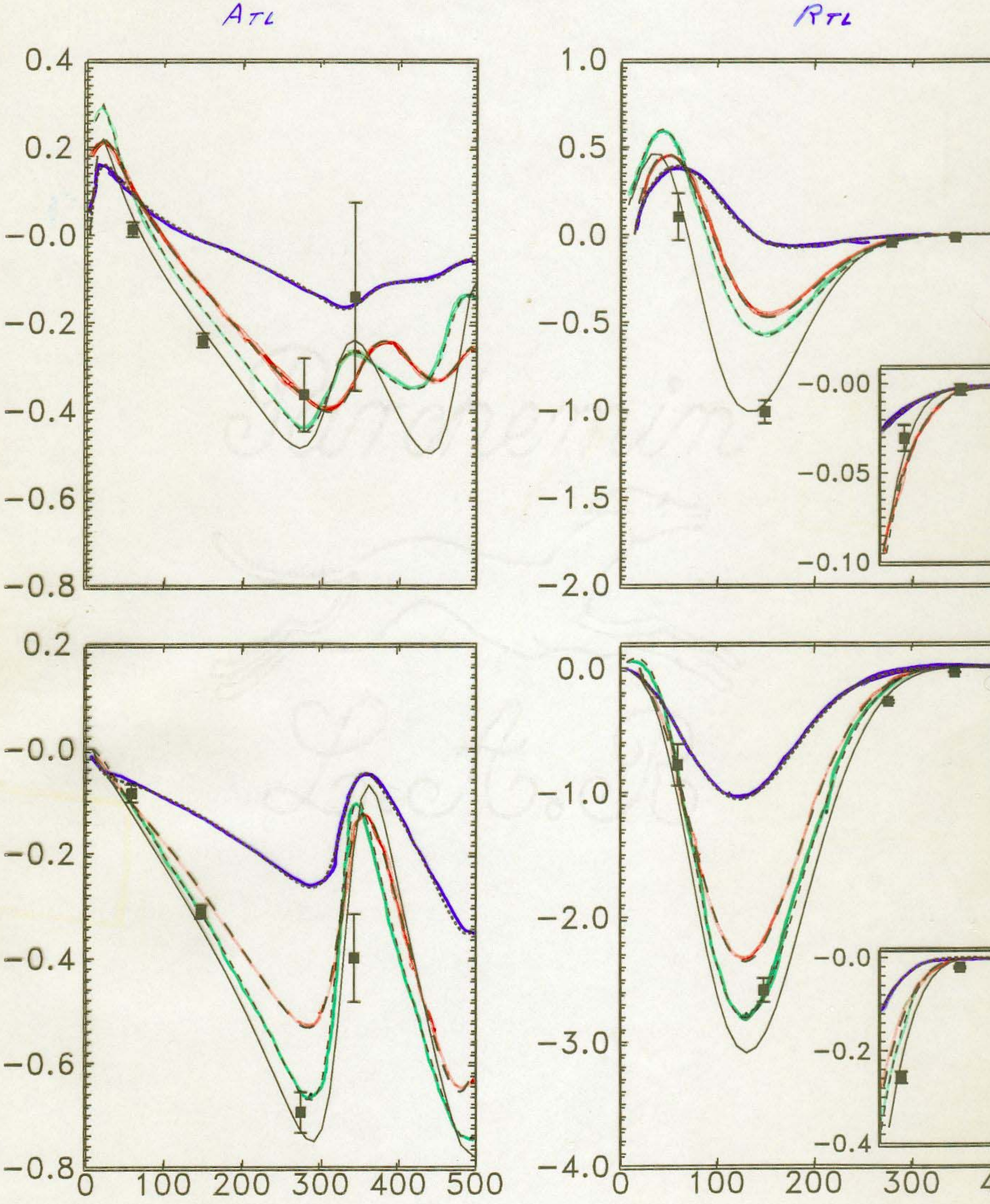

— nonrel. PRL 99

— ϕ_{nr} & rel. kin. PRL 00

Relativistic effects of three kinds in J_μ

1) Kinematical ~ higher $\vec{P}/M$ terms

2) Dynamical a) "increased absorption" in nuclear interior

b) enhancement of lower comp.

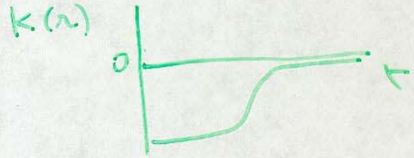

a) $\psi_{up} = K(r)\ \phi_{n.r.}(r)$

b) $\psi^{d.e.}_{down} = \left(\dfrac{\vec{\sigma}\cdot\vec{p}}{\widetilde{E}+\widetilde{M}} - \dfrac{\vec{\sigma}\cdot\vec{p}}{E+M}\right)\psi_{up}$

$$= \frac{V+S}{\widetilde{E}+\widetilde{M}}\left(\frac{\vec{\sigma}\cdot\vec{p}}{E+M}\psi_{up}\right)$$

$\Rightarrow$ smaller ρ's at Pm $\leq$ 300 MeV

larger ρ's at Pm $\geq$ 300 MeV

Gennuine rel. effects

larger effects in R_{LT} of $p_{1/2}$, $d_{3/2}$

SUPERSCALING IN NUCLEI: A SEARCH FOR SCALING FUNCTION BEYOND THE RELATIVISTIC FERMI GAS MODEL

We construct a scaling function $f(\psi')$ for inclusive electron scattering from nuclei within the Coherent Density Fluctuation Model (CDFM). The latter is a natural extension to finite nuclei of the Relativistic Fermi Gas (RFG) model within which the scaling variable ψ' was introduced by Donnelly and collaborators. The calculations show that the high-momentum components of the nucleon momentum distribution in the CDFM and their similarity for different nuclei lead to quantitative description of the superscaling in nuclei. The results are in good agreement with the experimental data for different transfer momenta showing superscaling for negative values of ψ', including those smaller than –1.

GCM Equations

$$\Psi(\mathbf{r}_1, ..., \mathbf{r}_A) = \int F(x_1, x_2, ...)\Phi(\mathbf{r}_1, ..., \mathbf{r}_A; x_1, x_2, ...)dx_1 dx_2...$$

– The Hill-Wheeler equation

$$\int [\mathcal{H}(x, x') - E\mathcal{I}(x, x')]F(x')dx' = 0$$

– The overlap and energy kernels

$$\mathcal{I}(x, x') = \langle \Phi(\{\mathbf{r}_i\}, x)|\Phi(\{\mathbf{r}_i\}, x')\rangle$$

$$\mathcal{H}(x, x') = \langle \Phi(\{\mathbf{r}_i\}, x)|\hat{H}|\Phi(\{\mathbf{r}_i\}, x')\rangle$$

– For many-fermion systems the kernels $\mathcal{I}(x, x')$ and $\mathcal{H}(x, x')$ peak strongly at $x \sim x'$

$$\mathcal{I}(x, x') \simeq \mathcal{I}(x, x)\mathcal{G}(x - x')$$

$$\mathcal{H}(x, x') \simeq \mathcal{H}(x, x)\mathcal{G}(x - x')$$

– Delta-function approximation

$$\mathcal{I}(x, x') \to \delta(x - x')$$

$$\mathcal{H}(x, x') \to -\frac{\hbar^2}{2m_{eff}}\delta''(x - x') + V\left(\frac{x + x'}{2}\right)\delta(x - x')$$

$$\int_0^\infty |F(x)|^2 dx = 1$$

$$\rho(\mathbf{r},\mathbf{r}') = \int_0^\infty dx |F(x)|^2 \rho_x(\mathbf{r},\mathbf{r}')$$

$$W(\mathbf{r},\mathbf{k}) = \int_0^\infty dx |F(x)|^2 W_x(\mathbf{r},\mathbf{k})$$

$$W_x(\mathbf{r},\mathbf{k}) = \frac{4}{(2\pi)^3}\Theta(x - |\mathbf{r}|)\Theta(k_F(x) - |\mathbf{k}|)$$

$$\rho(\mathbf{r}) = \int d\mathbf{k} W(\mathbf{r},\mathbf{k}) = \int_0^\infty dx |F(x)|^2 \frac{3A}{4\pi x^3}\Theta(x - |\mathbf{r}|)$$

$$\begin{aligned} n(\mathbf{k}) &= \int d\mathbf{r} W(\mathbf{r},\mathbf{k}) = \tfrac{4}{(2\pi)^3}\int_0^\infty dx |F(x)|^2 \tfrac{4\pi x^3}{3}\Theta(k_F(x) - |\mathbf{k}|) \\ &= \tfrac{4}{(2\pi)^3}\int_0^{\alpha/k} dx |F(x)|^2 \tfrac{4}{3}\pi x^3 \end{aligned}$$

$$\int \rho(\mathbf{r}) d\mathbf{r} = A; \quad \int n(\mathbf{k}) d\mathbf{k} = A$$

$$|F(x)|^2 = -\frac{1}{\rho_0(x)} \left.\frac{d\rho(r)}{dr}\right|_{r=x}, \quad (\text{at } d\rho(r)/dr \le 0)$$

$$f_{CDFM}(\psi') = \int_0^\infty dx|F(x)|^2 f_{RFG}(\psi'_x(\psi')),$$

$$\psi'_x(\psi') = [k_F/k_F(x)]\psi'$$

$$k_F(x) = \left(\frac{3\pi^2}{2}\rho_0(x)\right)^{1/3} \equiv \frac{\alpha}{x} \quad \text{with} \quad \alpha = \left(\frac{9\pi A}{8}\right)^{1/3} \simeq 1.52A^{1/3}$$

$$k_F = \int_0^\infty dx k_F(x)|F(x)|^2 = \alpha \int_0^\infty dx \frac{1}{x}|\mathcal{F}(x)|^2$$

$$\begin{aligned} f(\psi') \; &= \; \textstyle\int_0^{\alpha/(k_F|\psi'|)} dx|F(x)|^2 \; \frac{3}{4} \; \left[1 - \left(\frac{k_F x\psi'}{\alpha}\right)^2\right] \\ &\times \; \left\{1 + \left(\frac{x m_N}{\alpha}\right)^2 \left(\frac{k_F x\psi'}{\alpha}\right)^2 \left[2 + \left(\frac{\alpha}{x m_N}\right)^2 - 2\sqrt{1 + \left(\frac{\alpha}{x m_N}\right)^2}\right]\right\} \end{aligned}$$

Table 1: Values of the parameters R and b (in fm) used in the calculations and the results for k_F (in fm^{-1}) obtained in the CDFM.

Nuclei	R	b	k_F
^{4}He	1.710	0.290	1.201
^{12}C	2.470	0.420	1.200
^{27}Al	3.070	0.519	1.267
^{56}Fe	4.111	0.558	1.270
^{197}Au	6.419	0.449	1.335

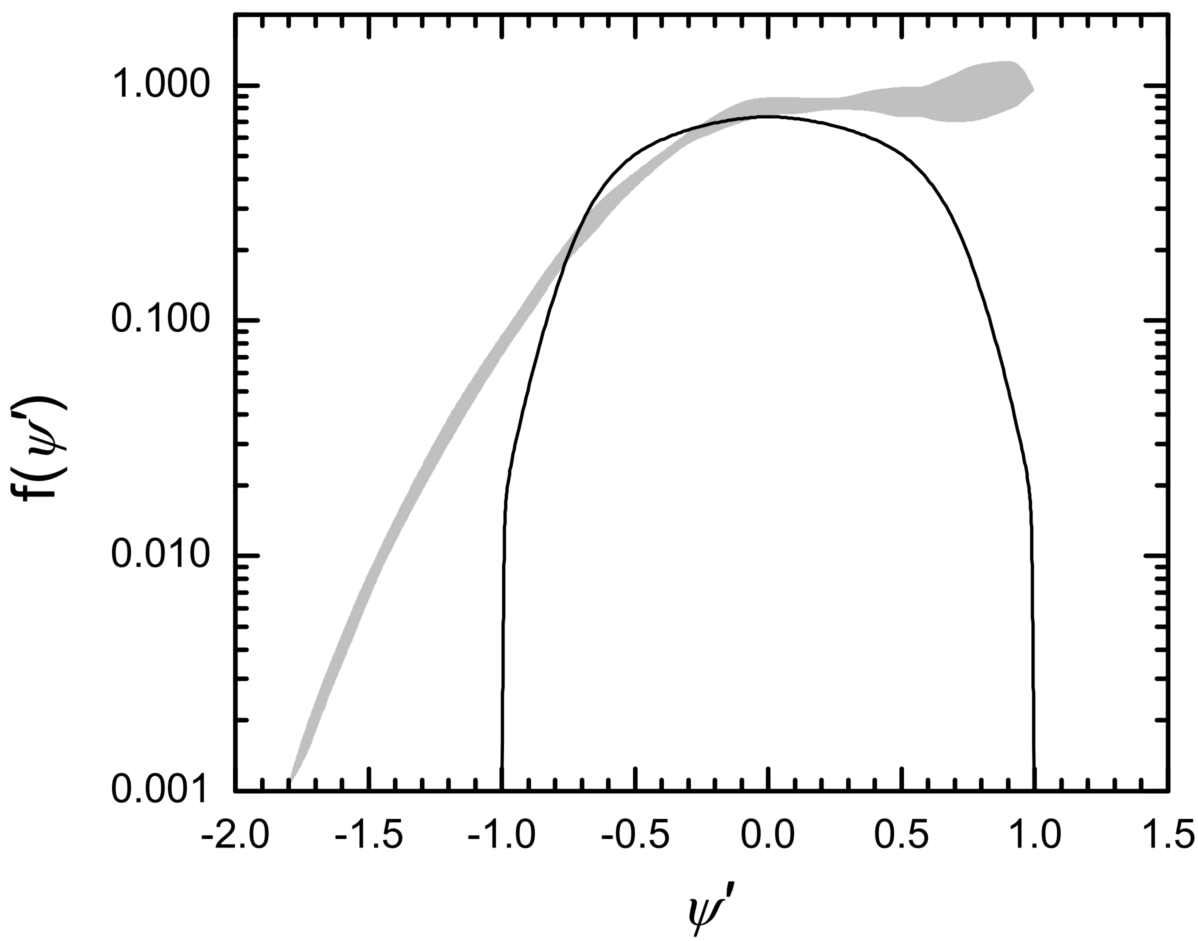

FIG. 1: Superscaling behaviour of inclusive electron-scattering. The grey area represents experimental data for ^{4}He, ^{12}C, ^{27}Al and ^{197}Au at $q = 1000$ MeV/c. The solid line is the RFG scaling function calculated with $k_F = 1.191$ fm^{-1}.

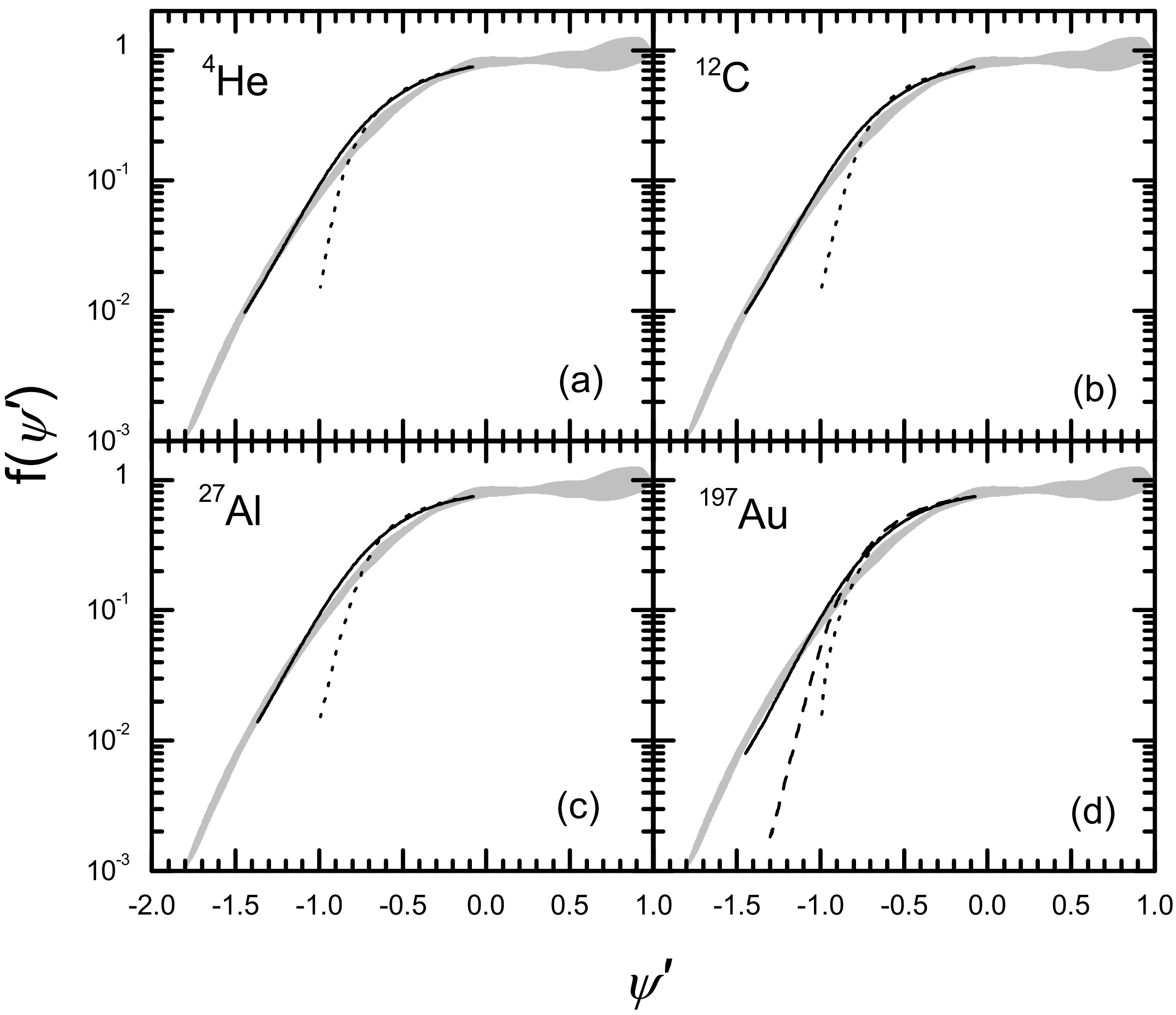

FIG. 2: Results for the scaling function in the CDFM (solid line) calculated at $q = 1000$ MeV/c and for ^{4}He, ^{12}C, ^{27}Al and ^{197}Au (with $b = 1.0$ fm for the latter) compared with the data (grey area). The dotted line is the RFG result. The dashed line in the case of ^{197}Au corresponds to the CDFM result with $b = 0.449$ fm.

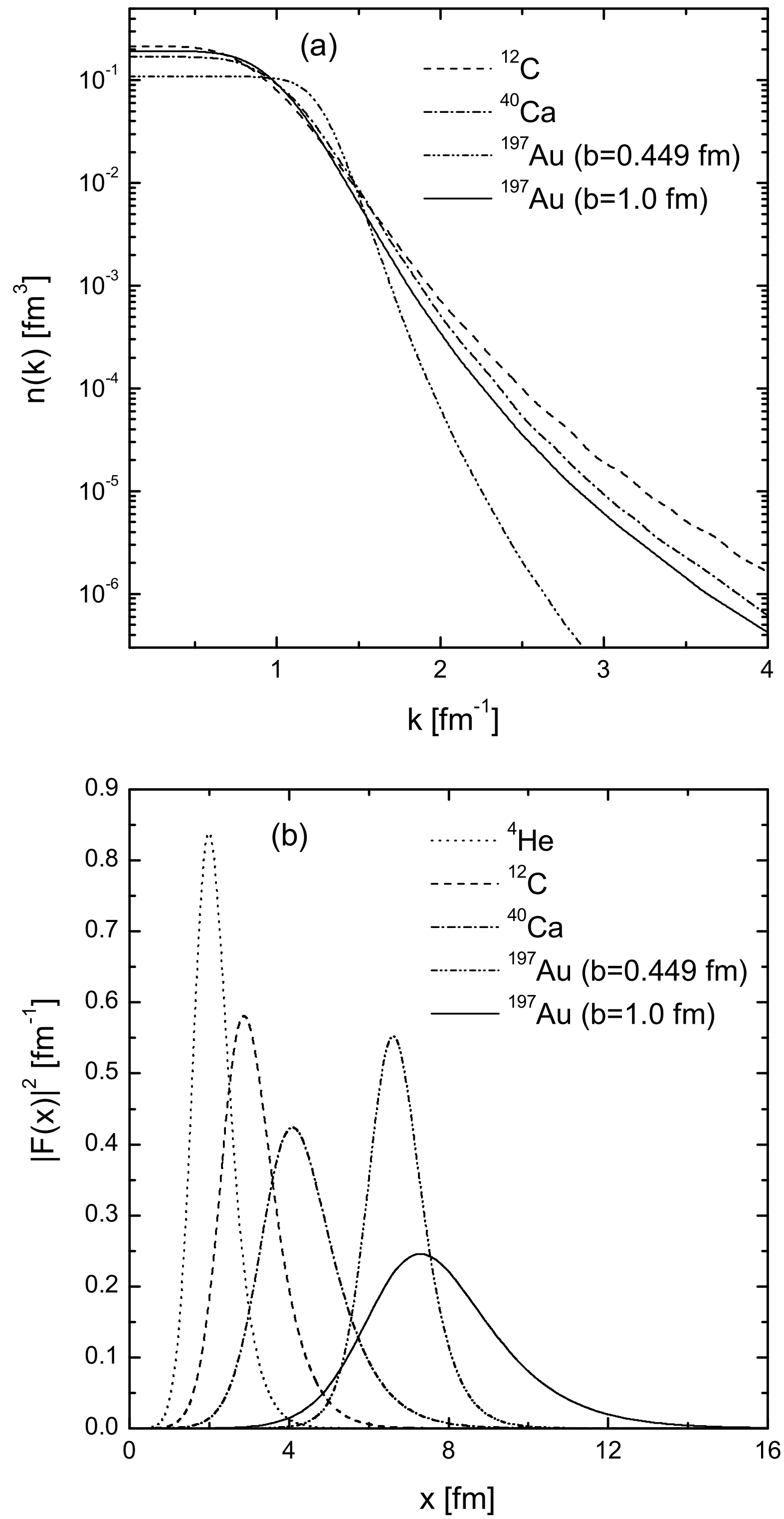

FIG. 3: (a) Nucleon momentum distribution $n(k)$ calculated in the CDFM for ^{12}C, ^{40}Ca and ^{197}Au (for the latter with $b = 0.449$ fm and $b = 1.0$ fm); (b) The weight function $|F(x)|^2$ of the CDFM calculated for ^{4}He, ^{12}C, ^{40}Ca and ^{197}Au (for the latter with $b = 0.449$ fm and $b = 1.0$ fm).

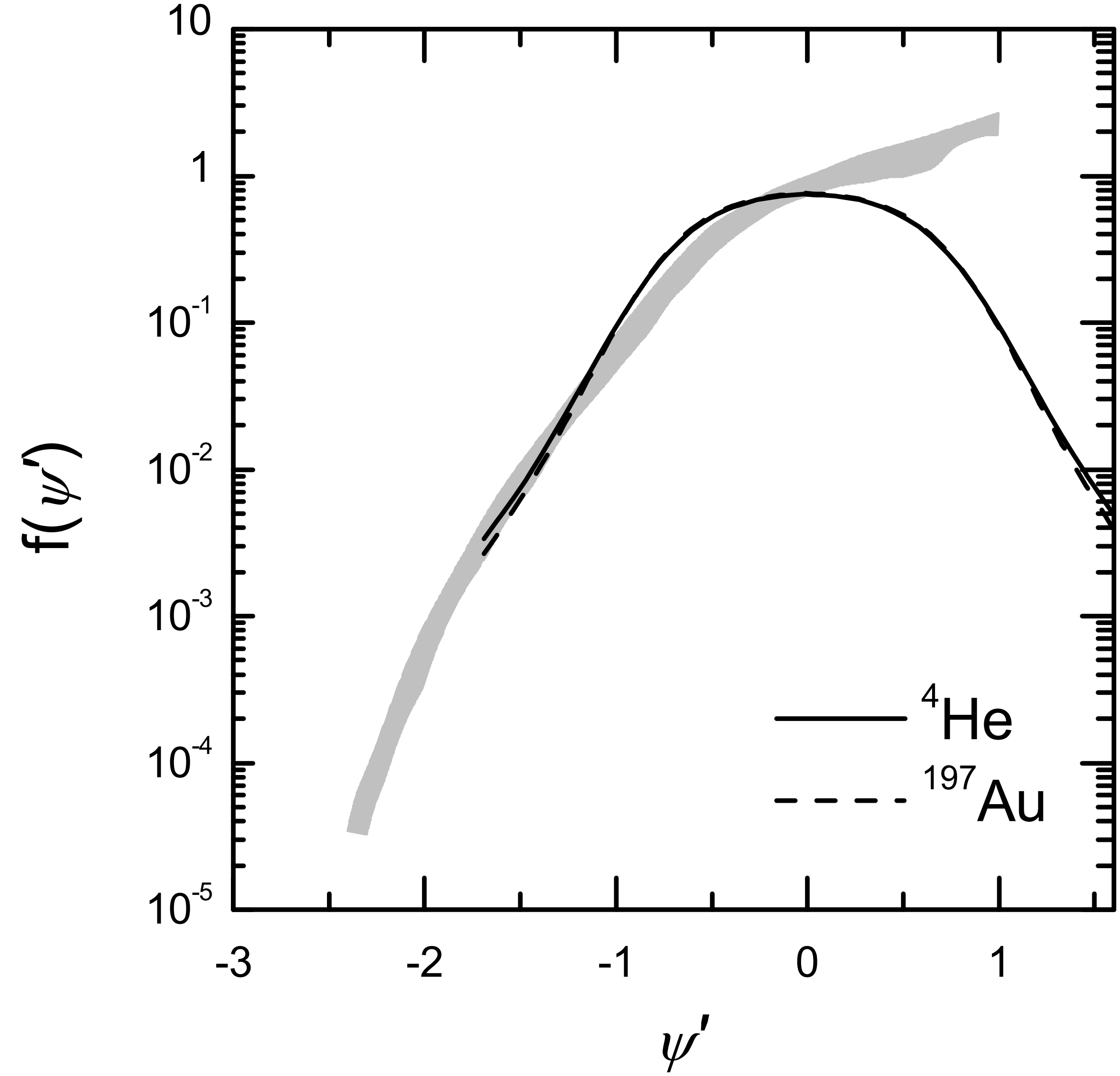

FIG. 4: Results of the CDFM for the superscaling functions of ^{4}He (solid line) and ^{197}Au (dashed line) at $q = 1650$ MeV/c compared with the experimental data (grey area).

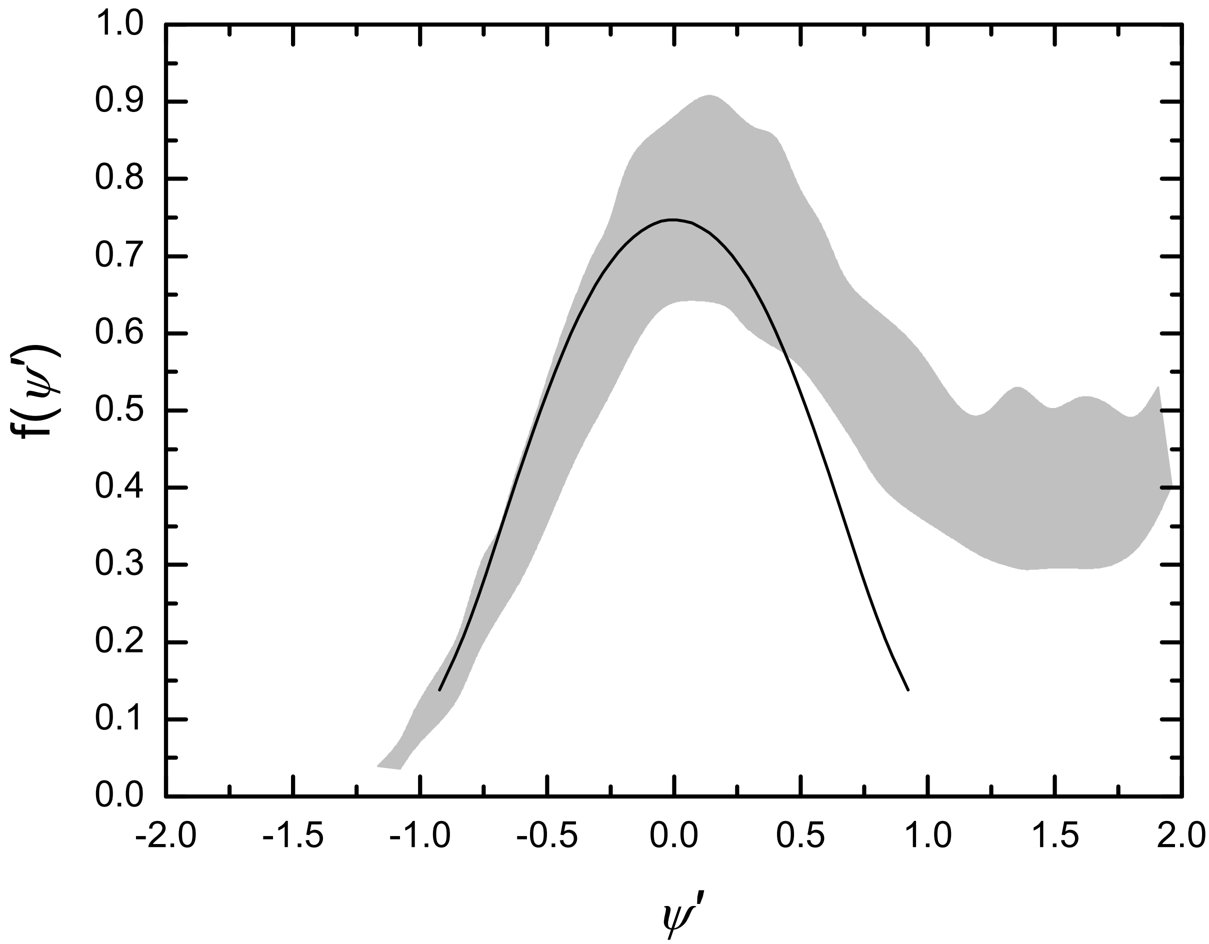

FIG. 5: Results of the CDFM for the superscaling function of ^{12}C at $q = 500$ MeV/c (solid line) compared with the experimental data (grey area) for q in the interval from 500 to 600 MeV/c.

In summary, the message is:

1) ^{3}He is an optimal nuclear system in what concerns "exact" treatment of correlations. Recent data on ^{3}He(e, e'p)^{2}H seem to show higher momentum tails than theory, which must then be atributed to relativistic and two-body current effects.

2) Electron induced proton knock-out from last bound orbital in Pb is an optimal case for fully relativistic one-body current, and good agreement between theory and experiment is obtained with a spectroscopic factor of 7.8, which implies an overall 20–30 % effect of correlations other than those contained in the r.m.f.

3) Study of superscaling and scaling function is the optimal probe of the high momentum tail of nucleon momentum distribution.